Liquid Crystal Dendrimers

Self-Assembly of Semifluorinated Janus-Dendritic Benzamides into Bilayered Pyramidal Columns**

Virgil Percec, Mohammad R. Imam, Tushar K. Bera, Venkatachalapathy S. K. Balagurusamy, Mihai Peterca, and Paul A. Heiney*

Amphiphilic dendrons that adopt the shape of a disk or disk fragment can self-assemble into supramolecular columns which self-organize into *p6mm* hexagonal or *p2mm* and *c2mm* rectangular 2D periodic assemblies.[1,2] The apex of such dendrons generates the hollow[1l] or occupied[1a–k] functional core of the supramolecular column (Figure 1a). Twin-tapered dendritic benzamides self-assemble into supramolecular columns generated by an orthogonal hydrogen-bonded stack of dendritic benzamide units (Figure 1b).[3] These supramolecular columns self-organize into periodically ordered *p6mm* hexagonal assemblies or co-assemble into more complex hexagonal superlattices.[3] Amphiphilic dendrons that adopt the shape of a sphere fragment can self-assemble into spherical supramolecular dendrimers, which self-organize into periodic $Pm\bar{3}n$,[1d,h,4a–4c] $Im\bar{3}m$[4d–f] 3D cubic and $P4_2/mnm$ 3D tetragonal,[4g] and quasiperiodic 3D 12-fold symmetry-forbidden liquid quasicrystals.[4h] It was recently reported that semifluorination of the conical dendron $(3,4,5)^2$12G2-CO_2CH_3 yields the crownlike dendron $(3,4,5)^2$12F8G2-CO_2CH_3 as one of the two products.[5] This

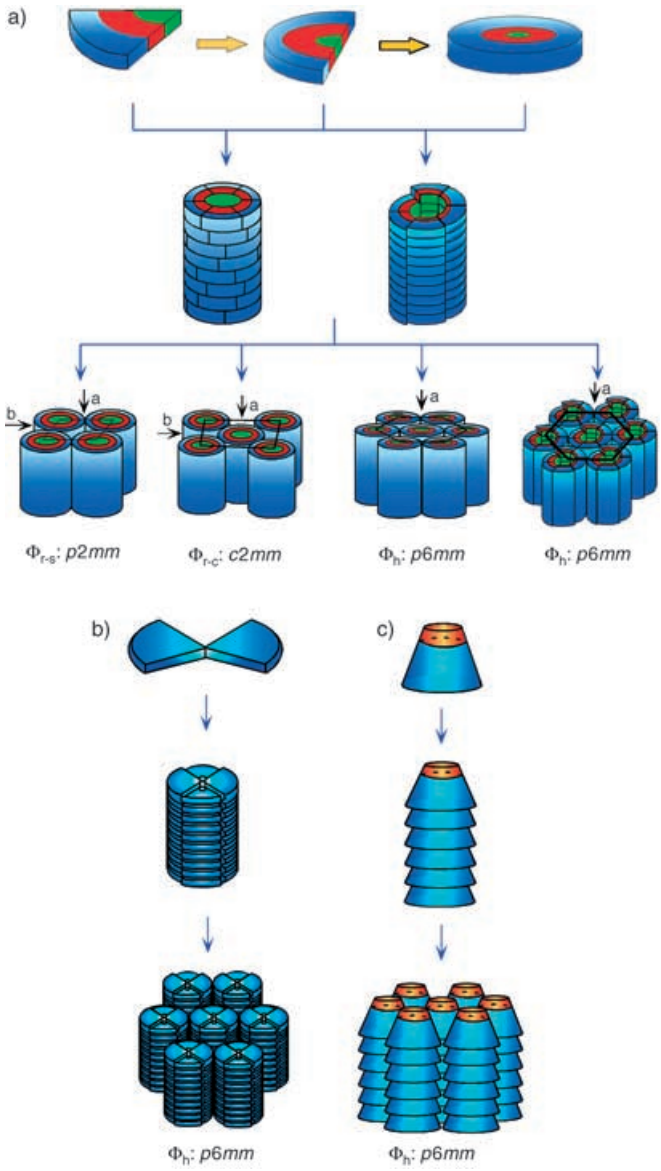

Figure 1. Self-assembly of building blocks based on a) flat, tapered dendrons into hollow and occupied supramolecular columns; b) twin dendrons into cylindrical columns; and c) crownlike dendrons into pyramidal columns and their subsequent self-organization into *p6mm* hexagonal columnar (Φ_h), *p2mm* simple rectangular columnar ($\Phi_{r\text{-}s}$), or *c2mm* centered rectangular columnar ($\Phi_{r\text{-}c}$) lattices.

[*] Prof. V. Percec, M. R. Imam, Dr. T. K. Bera, Dr. V. S. K. Balagurusamy
Roy & Diana Vagelos Laboratories, Department of Chemistry
Laboratory for Research on the Structure of Matter
University of Pennsylvania
Philadelphia, PA 19104-6323 (USA)
Fax: (+1) 215-573-7888
E-mail: percec@sas.upenn.edu
Dr. V. S. K. Balagurusamy, M. Peterca, Prof. P. A. Heiney
Department of Physics and Astronomy
Laboratory for Research on the Structure of Matter
University of Pennsylvania
Philadelphia, PA 19104-6396 (USA)

[**] Financial support by the National Science Foundation (DMR-9996288 and DMR-0102459) is gratefully acknowledged.

Supporting information for this article is available on the WWW under http://www.angewandte.org or from the author.

 DOI: 10.1002/ange.200501254

process changes the mode of self-assembly from a supramolecular sphere (for $(3,4,5)^2$12G2-CO_2CH_3) to a supramolecular pyramidal column for $(3,4,5)^2$12F8G2-CO_2CH_3 (Figure 1c). Herein, we report that semifluorination of one of the two dendrons of the twin-dendritic benzamides (that is, a benzamide containing two identical dendrons)[3b,c] changes the mode of self-assembly from a single-layer supramolecular column to an unprecedented bilayered pyramidal supramolecular column. The supramolecular pyramidal columns generated from these semifluorinated Janus-dendritic benzamides (that is, a benzamide containing two different dendrons) exhibit diameters more than twice as large as their nonfluorinated or semifluorinated twin-dendritic benzamide counterparts. Nonfluorinated Janus-dendritic benzamides continue to self-assemble like twin-dendritic benzamides.

Our study involved two nonfluorinated benzamides (3,4,5)12G1-(3,4,5)12G1-BzA **1** and (4-3,4,5)12G1-(4-3,4,5)12G1-BzA **3**, one fluorinated twin-dendritic benzamide (3,4,5)12F8G1-(3,4,5)12F8G1-BzA **2**, and a nonfluorinated Janus-dendritic benzamide (3,4,5)12G1-(4-3,4,5)12G1-BzA **4**. The synthesis, structural analysis, and mechanism of self-assembly of the two nonfluorinated twin-dendritic benzamides **1** and **3** were reported previously.[3b,c] Both **1** and **3** self-assemble into supramolecular columns by the orthogonal hydrogen-bonded stack mechanism outlined in Figure 1b. The fluorinated twin-dendritic benzamide **2** was synthesized with the procedure used for the corresponding nonfluorinated twin-dendritic benzamides[3b] (see Supporting Information). The semifluorinated twin-dendritic benzamides self-assemble into supramolecular columns by a mechanism similar to that of the nonfluorinated twin-dendritic benzamides (Figure 1b). The phase transitions for these three twin-dendritic benzamides, identified by a combination of

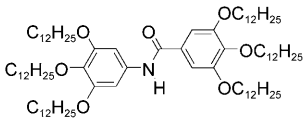

1

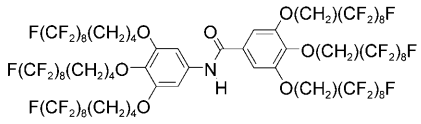

2

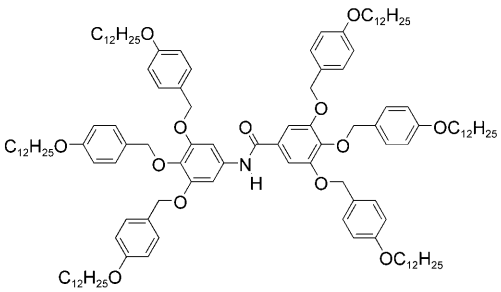

3

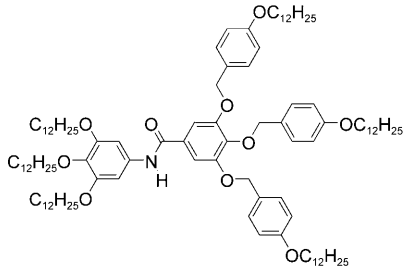

4

Table 1: Thermal analysis of the supramolecular dendrimers self-assembled from twin-dendritic and Janus-dendritic benzamides.[a]

Compound		Heating			Cooling	
	Phase Transition	T [°C]	ΔH [kcal mol^{-1}]	Phase Transition	T [°C]	ΔH [kcal mol^{-1}]
1	$k \rightarrow \Phi_h$	76.9	35.04	$i \rightarrow \Phi_h$	112.7	−0.77
	$\Phi_h \rightarrow i$	121.3	0.63	$\Phi_h \rightarrow k(\Phi_{r\text{-}c})$	47.1	−13.94
s.h.[b]	$k \rightarrow \Phi_h$	73.5	14.60			
	$\Phi_h \rightarrow i$	120.6	0.42			
2	$k \rightarrow \Phi_h$	134.9	16.28	$i \rightarrow \Phi_h$	146.5	−2.26
	$\Phi_h \rightarrow i$	150.1	2.38	$\Phi_h \rightarrow k$	49.9	−10.06
s.h.	$k_1 \rightarrow k_2$	104.6	−0.64			
	$k_2 \rightarrow \Phi_h$	134.8	16.65			
	$\Phi_h \rightarrow i$	149.8	2.29			
3	$k_1 \rightarrow k_2$	66.3	20.34	$i \rightarrow \Phi_h$	179.5	−2.54
	$k_2 \rightarrow \Phi_h$	101.0	11.16	$\Phi_h \rightarrow k$	78.3	−10.72
	$\Phi_h \rightarrow i$	182.8	2.43			
s.h.	$k_1 \rightarrow k_2$	−5.9	2.37			
	$k_2 \rightarrow \Phi_h$	101.5	12.41			
	$\Phi_h \rightarrow i$	181.9	2.76			
4	$k \rightarrow N_c$	45.7	8.63	$i \rightarrow \Phi_h$	138.3	−1.41
	$N_c \rightarrow \Phi_h$	56.3	2.81	$\Phi_h \rightarrow k$	34.9	−0.74
	$\Phi_h \rightarrow i$	141.6	1.62			
s.h.	$k \rightarrow \Phi_h$	48.5	0.91			
	$\Phi_h \rightarrow i$	141.6	1.61			
5	$k \rightarrow \Phi_h$	106.1	9.40	$i \rightarrow \Phi_h$	153.1	−1.88
	$\Phi_h \rightarrow i$	156.9	1.82	$\Phi_h \rightarrow k(\Phi_{r\text{-}c})$	69.8	−9.16
s.h.	$k \rightarrow \Phi_h$	105.8	9.95			
	$\Phi_h \rightarrow i$	156.5	2.03			
6	$k_1 \rightarrow k_2$	62.6	0.57	$i \rightarrow N_c$	72.2	−15.33
	$k_1 \rightarrow i$	105.6	23.11			
s.h.	$k \rightarrow N_c$	94.7	8.92			
	$N_c \rightarrow i$	101.7	0.89			
7	$k_1 \rightarrow k_2$	39.1	1.44	Φ_h dec $\rightarrow k$	131.2	−3.15
	$k_2 \rightarrow \Phi_{r\text{-}s}$	88.4	3.14			
	$\Phi_{r\text{-}s} \rightarrow \Phi_h$ dec[c]	137.3	3.16			
s.h.	$k \rightarrow \Phi_h$ dec	137.3	3.70			

[a] k: Crystalline; Φ_h: *p6mm* hexagonal columnar LC phase; i: isotropic; k($\Phi_{r\text{-}c}$): *c2mm* centered rectangular columnar crystalline; N_c: columnar nematic LC phase; $\Phi_{r\text{-}s}$: *p2mm* simple rectangular columnar LC phase. [b] s.h.: Data from the second heating. [c] The compound exhibits a decomposition temperature at 240.9 °C.

differential scanning calorimetry (DSC) and X-ray diffraction (XRD) experiments, are reported in Table 1. Their structural and retrostructural analysis by a combination of XRD, thermal optical polarized microscopy (TOPM), and molecular modeling experiments is reported in Table 2. Surprisingly, the nonfluorinated Janus-dendritic benzamide **4** also self-assembles into a supramolecular column by a mechanism similar to that of the twin-dendritic benzamides (Figure 1 b).

The semifluorinated Janus-dendritic benzamides (3,4,5)12G1-(3,4,5)12F8G1-BzA **5** and (4-3,4,5)12G1-(4-3,4,5)12F8G1-BzA **7** were synthesized from dendrons with identical structures, except one is semifluorinated and the other has hydrogenated alkyl groups on the periphery. Both dendritic benzamides self-assemble into supramolecular columns that self-organize in a *p6mm* columnar hexagonal (Φ_h) liquid crystal (LC) lattice (Table 1 and Table 2). However, the diameter of the supramolecular column self-assembled from **5** is twice that of the column self-assembled from the twin-dendritic benzamides **1** and **2**. A similar result was observed for the diameter of the supramolecular column self-assembled from **7**. The benzamide (3,4)12G1-(3,4,5)12F8G1-BzA **6** self-assembles into a less perfect supramolecular column with a diameter approximately twice as large as that of the column generated from **2** (Table 1 and Table 2). The less perfect supramolecular column produced by **6** self-organizes in a columnar nematic mesophase.

The XRD and TOPM textures of the columnar hexagonal lattices generated from nonfluorinated twin-dendritic benzamides are compared with those of semifluorinated Janus-dendritic benzamides in Figure 2 and Figure 3. Electron density calculations were performed to elucidate the origin of the difference between the diameters of the supramolecular columns self-organized from twin- and Janus-dendritic benzamides.

The Janus-dendritic benzamide **4**, which contains hydrogenated aliphatic chains, shows a strong and a very weak reflection in the XRD pattern recorded at 70 °C. The *d* spacings of these reflections are 27.4 Å and 15.9 Å, respectively (Table 2). The ratio of these *d* spacings is 1.72:1, which is very close to $\sqrt{3}$. This ratio demonstrates a Φ_h phase that exhibits only (10) and (11) reflections. Furthermore, these reflections give a column diameter of 31.7 Å. This is

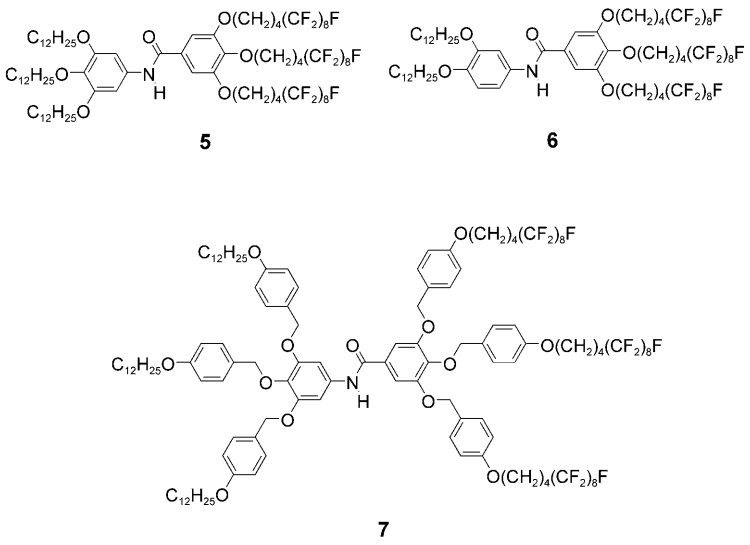

Table 2: Structural and retrostructural analysis of 2D lattices self-organized from twin- and Janus-dendritic benzamides.

Compound	*T* [°C]	LC Phase	*d* Spacings [Å] and Indices					Lattice Dimension or Column Diameter [Å][h]	ρ [g cm^{-3}] [i]	μ[j]
			d_{20}[a] d_{51}[b] d_{10}[c] d_{30}[d] d_{10}[e] d_{10}[f] d_{04}[g]	d_{11} d_{42} d_{11} d_{22} d_{11} d_{11} d_{30}	d_{31} d_{13} d_{20} d_{40} d_{12} d_{31}	d_{40} d_{33} d_{21} d_{21} d_{15}	d_{22} d_{53}			
1	21	$\Phi_{r\text{-}c}$	22.8[a]	18.6	–	11.3	–	a = 45.5	–	–
		$\Phi_{r\text{-}c}$	8.3[b]	7.6	6.8	–	–	b = 20.5	–	–
	90	Φ_h	21.7[c]	12.8	–	–	–	25.3 ± 0.4	0.98	1.8
2	78	Φ_h	28.8[c]	16.7	14.3	10.9	–	33.2 ± 0.2	–	–
3	94	Φ_h	29.2[c]	17.2	–	–	–	34.1 ± 0.5	0.93	2.1
4	50	N_c	42.5[e]	23.9	–	–	–	48.4	–	–
	70	Φ_h	27.4[c]	15.9	–	–	–	31.7	0.99	2.3
5	19	$\Phi_{r\text{-}c}$	45.3[a]	–	24.8	–	20.4	a = 90.3	–	–
		$\Phi_{r\text{-}c}$	16.6[b]	15.6	–	13.1	11.7	b = 44.7	–	–
	120	Φ_h	51.9[c]	–	25.4	19.2	–	59.0 ± 1.0	1.57	9.2
		Φ_h	16.9[d]	–	–	–	–	–	–	–
6	50	N_c	45.9[e]	–	–	–	–	53.0	–	–
7	100	$\Phi_{r\text{-}s}$	66.1[f]	56.1	41.3	32.4	–	a = 66.9	–	–
		$\Phi_{r\text{-}s}$	22.6[g]	21	21.7	20.1	–	b = 106.1	–	–
	150	Φ_h	64.8[c]	–	32.6	24.5	–	75.0	1.30	9.6
		Φ_h	21.6[d]	18.8	16.3	–	–	–	–	–

[a] *d* Spacings with indices for a *c2mm* simple rectangular columnar lattice ($\Phi_{r\text{-}c}$): (20), (11), (31), (40), and (22); [b] for indices (51), (42), (13), (33), and (53). [c] *d*-Spacings with indices for a *p6mm* hexagonal columnar lattice (Φ_h): (10), (11), (20), and (21); [d] for indices (30), (22), and (40); the *d*-spacing ratios are as expected for the 2D hexagonal columnar lattice: $d_{10}/d_{11}/d_{20}/d_{21}/d_{30}/d_{22}/d_{40} = 1:(1/\sqrt{3}):(1/\sqrt{4}):(1/\sqrt{7}):(1/\sqrt{9}):(1/\sqrt{12}):(1/\sqrt{16})$. [e] *d* Spacings with indices for a nematic columnar lattice (N_c). [f] *d*Spacings with indices for a *p2mm* simple rectangular columnar lattice ($\Phi_{r\text{-}s}$): (10), (11), (12), and (21); [g] For indices (04), (30), (31), and (15). [h] For the Φ_h LC phase, lattice dimension *a* is the same as the column diameter; for $\Phi_{r\text{-}c}$ and $\Phi_{r\text{-}s}$ phases, lattice dimensions *a* and *b* are given. [i] Experimental density of the molecule in the LC phase. [j] Number of monodendrons per cylindrical stratum of the supramolecular column: $\mu = (\sqrt{3} N_A a^2 t \rho)/2M$; ($N_A = 6.022045 \times 10^{23}$ mol^{-1}, t = 7.2 Å = average column stratum height, ρ = average density of the molecule in the LC phase, a = lattice dimension, M = molar mass of the monodendron).

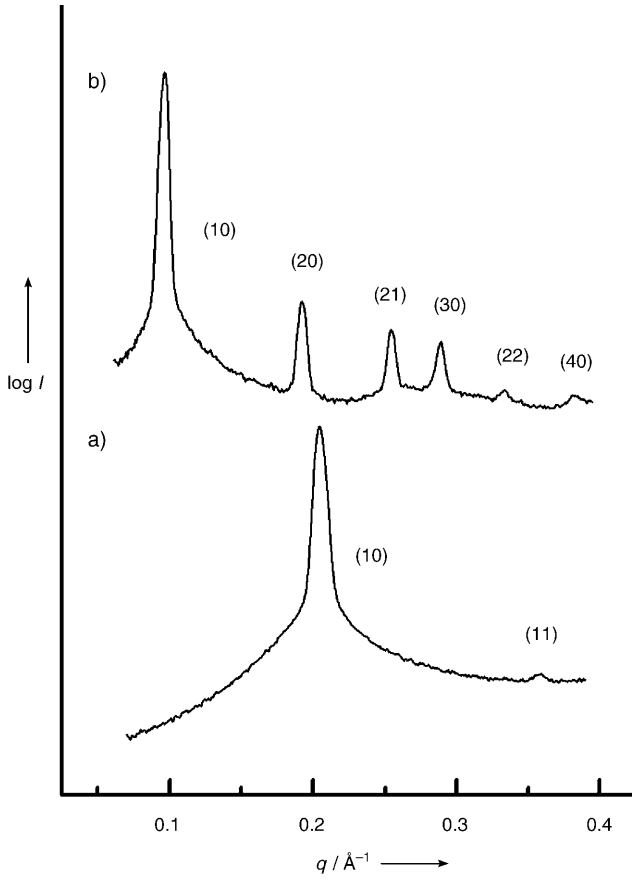

Figure 2. XRD pattern in the Φ_h phase of a) **3** and b) **7**. In b), the observed peaks shift to larger *d* spacings, which leads to a greater than twofold increase in column diameter.

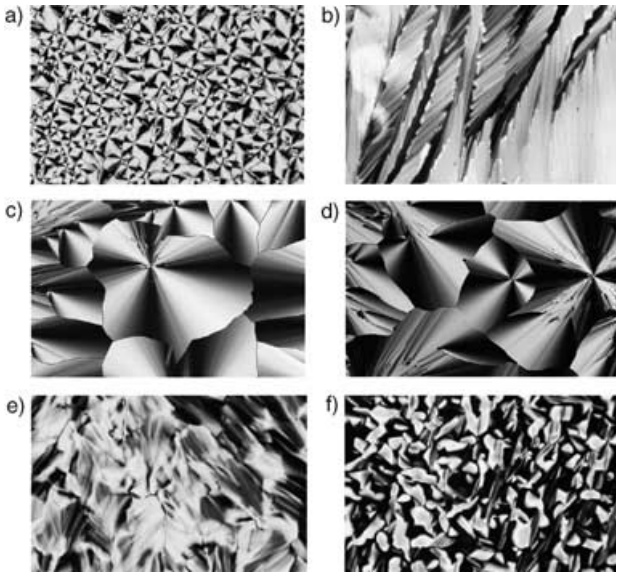

Figure 3. Representative TOPM textures of the hexagonal columnar (Φ_h) mesophase, obtained by cooling at a rate of 1 °C min^{-1} from isotropic phase of a) **1**; b) **2**; c) **3**; d) **4**; e) **5**; and f) **7**.

smaller than that of the twin-dendritic benzamide **3** (a = 34.1 Å, Figure 2a and Table 2), which forms an orthogonal stack of dendrons in its supramolecular column.[3c] However, the column diameter of the Janus benzamide **4** (a = 31.7 Å) is larger than that of the supramolecular column generated from the twin benzamide **1** (a = 25.3 Å).[3b] This indicates that the nonfluorinated Janus-dendritic benzamide **4** forms an orthogonal stack of dendrons in the column of its Φ_h phase that is similar to those of the columns self-assembled from nonfluorinated twin-dendritic benzamides **3** and **1**.

The twin-dendritic benzamide **2**, which contains only semifluorinated aliphatic chains, shows four reflections in the XRD pattern at 78 °C. They are indexed to the (10), (11), (20), and (21) peaks of a 2D Φ_h phase generated from columns with a diameter of 33.2 Å (Table 2). This diameter is substantially larger than that of the nonfluorinated twin-dendritic benzamide **1**. However, the column diameter is close to that of the supramolecular column of the nonfluorinated Janus-dendritic benzamide **4**, evidence that its corresponding supramolecular column is constructed from an orthogonal stack of building blocks.

The semifluorinated Janus-dendritic benzamide **7**, which contains hydrogenated aliphatic chains in one dendron and semifluorinated aliphatic chains in the other, forms a Φ_h phase above 137.3 °C. The X-ray diffraction pattern at 150 °C shows the reflections (10), (20), (21), (30), (22), and (40) that index to a 2D Φ_h lattice with a column diameter of 75.0 Å (Figure 2b). This column diameter is about 2.2-fold larger than that of the twin-based column of **3** (a = 34.1 Å), suggesting that in the semifluorinated Janus column, the fluorinated aliphatic regions do not mix with the hydrogenated aliphatic regions as a result of a fluorophobic effect.[6] If they mixed, they would generate only an orthogonal stack with a column diameter expected to be very close to that of the nonfluorinated Janus-dendritic benzamide **4**. Similarly, the semifluorinated Janus-dendritic benzamide **5** self-assembles into a supramolecular column with a column diameter of 59 Å (Table 2), which is 2.3-fold larger than that of the corresponding nonfluorinated twin-dendritic benzamide, **1** (a = 25.3 Å). These results suggest that the semifluorinated Janus-dendritic benzamides **5** and **7** self-assemble into a bilayered disc or crown in which the semifluorinated regions are segregated from hydrogenated aliphatic regions, with the aromatic part of the molecules occupying the intermediate region between the core and the periphery. The disc or crownlike aggregate generates the supramolecular column. This arrangement contrasts with the orthogonal stack formed by nonfluorinated or semifluorinated twin-dendritic benzamides and by nonfluorinated Janus-dendritic benzamides.

Electron density profiles were computed with the aid of the integrated intensity data calculated from the X-ray diffraction peaks obtained in the Φ_h phase to visualize the molecular organization of the dendrons in various supramolecular columns (Figure 4).[4a] The XRD of the nonfluorinated Janus benzamide **4** in the Φ_h phase shows a very strong (10) peak and a very weak (11) peak that are expected from the orthogonal stacks formed by these molecules.[3c] The electron density profile computed with the phase choice "+ −" for these two reflections exhibits a maximum in the core. The maximum electron density of the core decreases towards the periphery of the column, becoming almost constant on the periphery (Figure 4a). This variation of the electron density

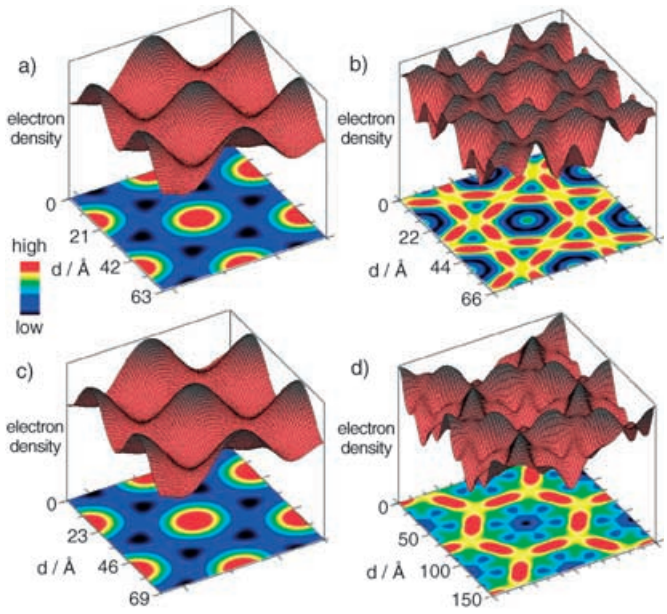

Figure 4. Electron density profiles and contour plots of the twin- and Janus-dendritic benzamides a) **4** showing the center of the supramolecular columns with high electron density (red) due to the aromatic parts; b) **2** with high electron density (red) in the periphery of the columns which corresponds to the semifluorinated aliphatic chains, and the low electron density (black), which corresponds to the hydrogenated aliphatic chains; c) **3** showing the center of the supramolecular columns with high electron density (red), which corresponds to the aromatic parts; and d) **7** with high electron density (red) in the periphery of the columns which corresponds to the semifluorinated aliphatic chains.

profiles is consistent with the nanophase segregation expected in these systems.[1c,d,4a] The maximum and the surrounding high electron density regions correspond to the aromatic portion of the molecules, and the near-constant peripheral regions represent the aliphatic part of the molecules from the orthogonal stack of the twin-dendritic benzamides. Similar electron density profiles were observed for the supramolecular columns self-assembled from the twin-dendritic benzamide **1**.

The semifluorinated twin-dendritic benzamide **2** shows additional reflections in the Φ_h phase that correspond to a strong (10) peak, a moderately strong (21) peak, a very weak (20) peak, and a weak (11) peak. The observation of a moderately strong (21) peak rather than a sequence of higher order peaks with decreasing intensity suggests that the semifluorinated aliphatic chains of the molecules occupy the peripheral regions of the columns. The electron density profiles computed with the phases "$- - + +$" for the peaks (10), (11), (20), and (21), respectively, show high and nearly constant electron density regions on the periphery of the columns (Figure 4b). They also show an intermediate electron density region near the core of the columns that corresponds to the aromatic portions. As one moves toward the periphery from the aromatic regions of the column, the electron density reaches a minimum and then rises toward the semifluorinated regions on the periphery. The regions surrounding the minima in the electron density correspond to the hydrogenated aliphatic part of the molecule. Notably, the electron density profile is similar to that observed in the Φ_h phase of a pyramidal columnar supramolecular dendrimer with semifluorinated aliphatic chains that was reported previously.[5a]

The electron density profiles of the twin-dendritic benzamide **3** is shown in Figure 4c. These profiles show maximum electron density in the center of the columns corresponding to the aromatic regions and low electron density corresponding to the aliphatic region in the periphery. The semifluorinated Janus-dendritic benzamide **7** shows the reflections (10), (20), (21), (30), (22), and (40). Whereas the peak with the strongest intensity is (10), the intensities of (20) and (30) peaks are higher than that of the (21) peak (Figure 2b). This is consistent with the semifluorinated aliphatic chains occupying the peripheral region of the column. Accordingly, the electron density profiles for the phases "$- + - - + -$" has high electron density in the peripheral region of the column and low electron density in the central region of the column (Figure 4d). Starting from the center of the column, the electron density increases from the lowest value to a small local maximum that corresponds to the aromatic part of the molecules. As one moves closer to the periphery from the aromatic region, the electron density decreases slightly owing to the hydrogenated part of the semifluorinated aliphatic chains. Therefore, the electron density profiles are consistent with the bilayered columnar structure containing the hydrogenated aliphatic chains in the core and the semifluorinated aliphatic chains in the periphery with the aromatic part occupying the intermediate region. Molecular models of the bilayered supramolecular columns obtained from small- and wide-angle XRD of oriented fibers are shown in Figure 5,

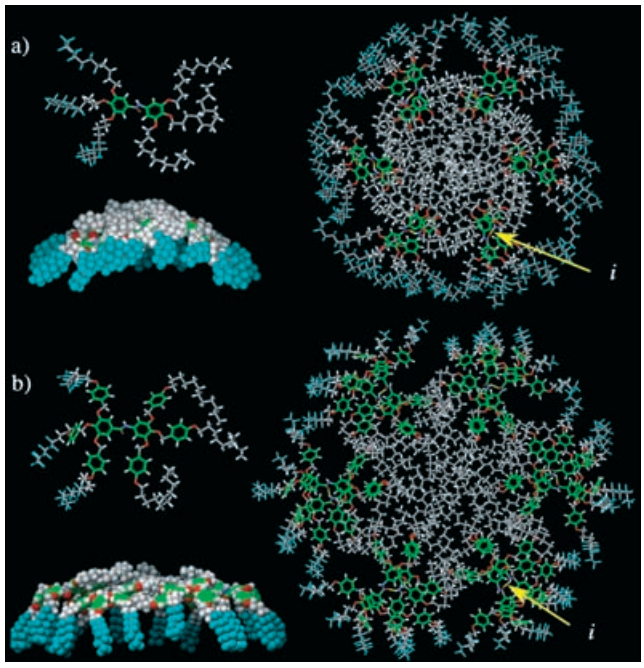

Figure 5. Structures of a) **5** and b) **7**. Top left: single dendron with the semifluorinated tails in blue; bottom left: space-filling side view of one crownlike layer; right: top view of two consecutive crownlike layers (*i* indicates the hydrogen bonding between layers).

Figure 6, and Figure 7. These models illustrate the location of the nonfluorinated alkyl chains in the central region of the column and the perfluorinated regions in the periphery of the column. Nonorthogonal hydrogen bonding is available in the crownlike stratum of the pyramidal column (Figure 5 and Figure 6). *N*-methylation of the –NH– groups of the Janus-dendritic benzamides almost destroys the pyramidal columnar assembly. The *N*-methylated Janus-benzamide derivative **5** displays a monotropic crystalline *p2mm* simple rectangular phase before melting at 67 °C (see Supporting Information). The crystals of its precursor benzamide **5** melt into a Φ_h phase at 106 °C, followed by isotropization at 157 °C (Table 1). The behavior of the latter demonstrates that hydrogen bonding is responsible for the formation of the LC phases of the Janus-dendritic benzamides.

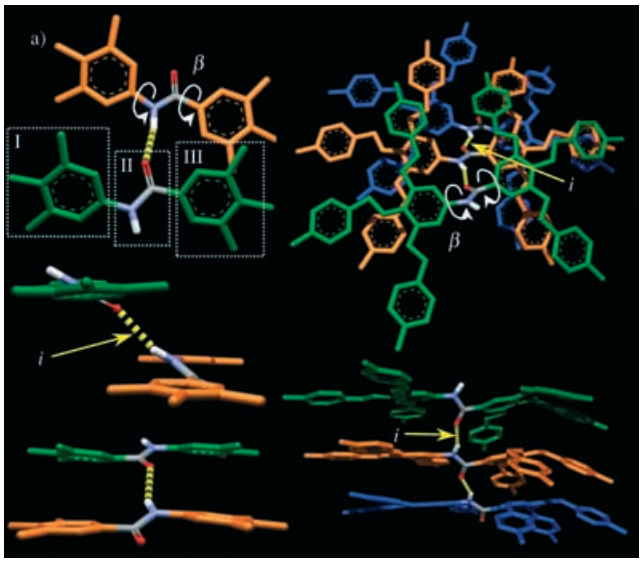

Figure 6. Hydrogen-bonding details for Janus benzamides a) **5** and b) **7**; only the aromatic regions are shown, with each dendron molecule colored differently. The formation of hydrogen bonds (*i*) requires a benzamide torsion angle (β) of about 30°, as the layer spacing is approximately 4.5–5.0 Å. Top left: dihedral angles between planes I and II, approximately 30°; between planes II and III, approximately 30° (Ref. [7]); and between planes I and III, 0°. The dihedral angle between planes I and III was chosen to be 0° instead of 62.6°, as reported in Ref. [7], to decrease the steric constrains and to facilitate better packing.

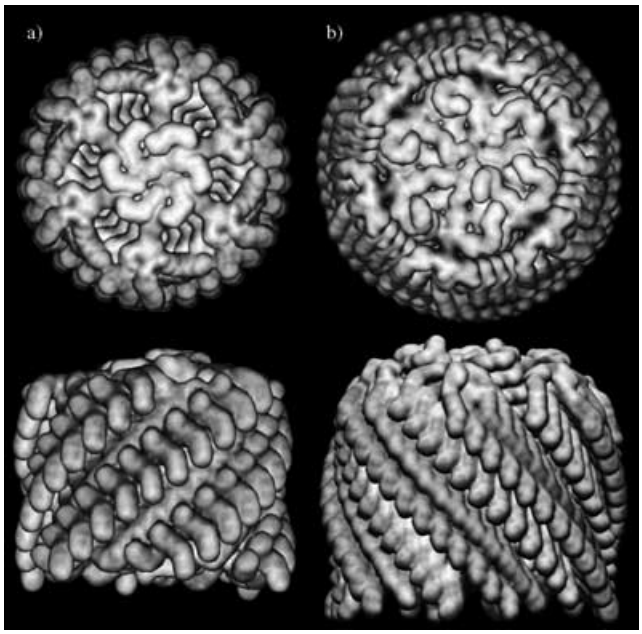

Figure 7. Supramolecular assembly models of a) **5** and b) **7**, indicating the higher electron density on the semifluorinated periphery and the short-range helical order of the supramolecular assembly.

In conclusion, the selective attachment of nonfluorinated aliphatic chains on one dendron and semifluorinated aliphatic chains on the other dendron of the twin-tapered dendritic benzamides generates semifluorinated Janus-dendritic benzamides. These, in turn, self-assemble into supramolecular pyramidal columns that exhibit diameters more than double those of the columns generated from nonfluorinated or semifluorinated twin-dendritic benzamides. This new mode of self-assembly of the semifluorinated Janus-dendritic benzamides results from the tendency of the semifluorinated aliphatic chains to segregate from the hydrogenated aliphatic chains. Aside from providing an unusual example of the fluorophobic effect in self-assembly[8,9] and the second example of supramolecular pyramidal dendrimers[5a,b] self-assembled from supramolecular crowns, this novel bilayered supramolecular pyramidal columnar structure opens numerous new strategies for the construction of complex supramolecular nanosystems.[2m,n,10] This initiates a new direction in the area of Janus-derived supramolecular liquid crystals,[2h,i] complements pyramidal mesophases generated from covalent crownlike molecules,[11] and raises the question about the generality of this concept.

Received: April 10, 2005
Published online: July 1, 2005

Keywords: amides · dendrimers · liquid crystals · self-assembly · supramolecular chemistry

[1] a) V. Percec, G. Johansson, J. Heck, G. Ungar, S. V. Batty, *J. Chem. Soc. Perkin Trans. 1* **1993**, 1411–1420; b) G. Johansson, V. Percec, G. Ungar, D. Abramic, *J. Chem. Soc. Perkin Trans. 1* **1994**, 447–459; c) V. Percec, G. Johansson, G. Ungar, J. Zhou, *J. Am. Chem. Soc.* **1996**, *118*, 9855–9866; d) S. D. Hudson, H.-T. Jung, V. Percec, W.-D. Cho, G. Johansson, G. Ungar, V. S. K. Balagurusamy, *Science* **1997**, *278*, 449–452; e) V. Percec, W.-D. Cho, P. E. Mosier, G. Ungar, D. J. P. Yeardley, *J. Am. Chem. Soc.* **1998**, *120*, 11061–11070; f) V. Percec, W.-D. Cho, G. Ungar, D. J. P. Yeardley, *Angew. Chem.* **2000**, *112*, 1661–1666; *Angew. Chem. Int. Ed.* **2000**, *39*, 1597–1602; g) V. Percec, W.-D. Cho, G. Ungar, *J. Am. Chem. Soc.* **2000**, *122*, 10273–10281; h) V. Percec, W.-D. Cho, G. Ungar, D. J. P. Yeardley, *J. Am. Chem. Soc.* **2001**, *123*, 1302–1315; i) V. Percec, W.-D. Cho, G. Ungar, D. J. P. Yeardley, *Chem. Eur. J.* **2002**, *8*, 2011–2025; j) V. Percec, M Glodde, T. K. Bera, Y. Miura, I. Shiyanovskaya, K. D. Singer, V. S. K. Balagurusamy, P. A. Heiney, I. Schnell, A. Rapp, H.-W. Spiess, S. D. Hudson, H. Duan, *Nature* **2002**, *419*, 384–387; k) V. Percec, C. M. Mitchell, W.-D. Cho, S. Uchida, M. Glodde, G. Ungar, X. Zeng, Y. Liu, V. S. K. Balagurusamy, P. A. Heiney, *J. Am. Chem. Soc.* **2004**, *126*, 6078–6094; l) V. Percec, A. E.

Dulcey, V. S. K. Balagurusamy, Y. Miura, J. Smidrkal, M. Peterca, S. Nummelin, U. Edlund, S. D. Hudson, P. A. Heiney, H. Duan, S. N. Magonov, S. A. Vinogradov, *Nature* **2004**, *430*, 764 – 768.

[2] a) D. J. Pesak, J. S. Moore, *Angew. Chem.* **1997**, *109*, 1709 – 1712; *Angew. Chem. Int. Ed. Engl.* **1997**, *36*, 1636 – 1639; b) H. Meier, M. Lehmann, *Angew. Chem.* **1998**, *110*, 666 – 669; *Angew. Chem. Int. Ed.* **1998**, *37*, 643 – 645; c) M. Marcos, A. Omenat, J. L. Serrano, *C. R. Chim.* **2003**, *6*, 947 – 957; d) M. Marcos, R. Gimenez, J. L. Serrano, B. Donnio, B. Heinrich, D. Guillon, *Chem. Eur. J.* **2001**, *7*, 1006 – 1013; e) M. Suarez, J.-M. Lehn, S. C. Zimmerman, A. Skoulios, B. Heinrich, *J. Am. Chem. Soc.* **1998**, *120*, 9526 – 9532; f) T. Chuard, M.-T. Beguin, R. Deschenaux, *C. R. Chim.* **2003**, *6*, 959 – 962; g) M. W. P. L. Baars, S. H. M. Söntjens, H. M. Fischer, H. W. I. Peerlings, E. W. Meijer, *Chem. Eur. J.* **1998**, *4*, 2456 – 2466; h) I. M. Saez, J. W. Goodby, *Chem. Eur. J.* **2003**, *9*, 4869 – 4877; i) I. M. Saez, J. W. Goodby, *Chem. Commun.* **2003**, 1726 – 1727; j) M. Kimura, Y. Saito, K. Ohta, K. Hanabusa, H. Shirai, N. Kobayashi, *J. Am. Chem. Soc.* **2002**, *124*, 5274 – 5275; k) C. Kim, K. T. Kim, Y. Chang, H. H. Song, T.-Y. Cho, H.-J. Jeon, *J. Am. Chem. Soc.* **2001**, *123*, 5586 – 5587; l) B.-K. Cho, A. Jain, S. M. Gruner, U. Wiesner, *Science* **2004**, *305*, 1598 – 1601; m) C. Tschierske, *Curr. Opin. Colloid Interface Sci.* **2002**, *7*, 69 – 80; n) S. A. Ponomarenko, N. I. Boiko, V. P. Shibaev, *J. Polym. Sci. Part C* **2001**, *43*, 1 – 45.

[3] a) G. Ungar, D. Abramic, V. Percec, J. A. Heck, *Liq. Cryst.* **1996**, *21*, 73 – 86; b) V. Percec, C.-H. Ahn, T. K. Bera, G. Ungar, D. J. P. Yeardley, *Chem. Eur. J.* **1999**, *5*, 1070 – 1083; c) V. Percec, T. K. Bera, M. Glodde, Q. Fu, V. S. K. Balagurusamy, P. A. Heiney, *Chem. Eur. J.* **2003**, *9*, 921 – 935.

[4] a) V. S. K. Balagurusamy, G. Ungar, V. Percec, G. Johansson, *J. Am. Chem. Soc.* **1997**, *119*, 1539 – 1555; b) V. Percec, C.-H. Ahn, G. Ungar, D. J. P. Yeardley, M. Möller, S. S. Sheiko, *Nature* **1998**, *391*, 161 – 164; c) G. Ungar, V. Percec, M. N. Holerca, G. Johansson, J. A. Heck, *Chem. Eur. J.* **2000**, *6*, 1258 – 1266; d) D. J. P. Yeardley, G. Ungar, V. Percec, M. N. Holerca, G. Johansson, *J. Am. Chem. Soc.* **2000**, *122*, 1684 – 1689; e) H. Duan, S. D. Hudson, G. Ungar, M. N. Holerca, V. Percec, *Chem. Eur. J.* **2001**, *7*, 4134 – 4141; f) V. Percec, M. N. Holerca, S. Uchida, W. -D. Cho, G. Ungar, Y. Lee, D. J. P. Yeardley, *Chem. Eur. J.* **2002**, *8*, 1106 – 1117; g) G. Ungar, Y. Liu, X. Zeng, V. Percec, W.-D. Cho, *Science* **2003**, *299*, 1208 – 1211; h) X. Zeng, G. Ungar, Y. Liu, V. Percec, A. E. Dulcey, J. K. Hobbs, *Nature* **2004**, *428*, 157 – 160; i) G. H. Mehl, *Angew. Chem.* **2005**, *117*, 678 – 679; *Angew. Chem. Int. Ed.* **2005**, *44*, 672 – 673.

[5] a) V. Percec, M. Glodde, G. Johansson, V. S. K. Balagurusamy, P. A. Heiney, *Angew. Chem.* **2003**, *115*, 4474 – 4478; *Angew. Chem. Int. Ed.* **2003**, *42*, 4338 – 4342; b) D. A. Tomalia, *Nat. Mater.* **2003**, *2*, 711 – 712.

[6] For fundamental reports on fluorinated materials, see: a) B. E. Smart in *Organofluorine Chemistry. Principles and Commercial Applications* (Eds.: R. E. Banks, B. E. Smart, J. C. Tatlow), Plenum, New York, **1994**; b) *Modern Fluoropolymers* (Ed.: J. Scheirs), Wiley, New York, **1997**; c) D. F. Eaton, B. E. Smart, *J. Am. Chem. Soc.* **1990**, *112*, 2821 – 2823.

[7] S. Kashino, K. Ito, M. Haisa, *Bull. Chem. Soc. Jpn.* **1979**, *52*, 365 – 369.

[8] For examples of fluorinated molecules in self-assembly, see: a) G. W. Coates, A. R. Dunn, L. M. Henling, D. A. Dougherty, R. H. Grubbs, *Angew. Chem.* **1997**, *109*, 290; *Angew. Chem. Int. Ed. Engl.* **1997**, *36*, 248 – 251; b) W. J. Feast, P. W. Lövenich, H. Puschmann, C. Taliani, *Chem. Commun.* **2001**, *5*, 505 – 506; c) D. R. Dukeson, G. Ungar, V. S. K. Balagurusamy, V. Percec, G. Johansson, M. Glodde, *J. Am. Chem. Soc.* **2003**, *125*, 15974 – 15980.

[9] For examples of fluorinated compounds in self-organization, see: a) U. Dahn, C. Erdelen, H. Ringsdorf, R. Festag, J. H. Wendorff, P. A. Heiney, N. C. Maliszewskyj, *Liq. Cryst.* **1995**, *19*, 759; b) G. Johansson, V. Percec, G. Ungar, K. Smith, *Chem. Mater.* **1997**, *9*, 164 – 175; c) V. Percec, D. Schlueter, G. Ungar, *Macromolecules* **1997**, *30*, 645 – 648; d) F. Guittard, E. T. de Givenchy, S. Geribaldi, A. Cambon, J. *Fluorine Chem.* **1999**, *100*, 85 – 96; e) X. H. Cheng, S. Diele, C. Tschierske, *Angew. Chem.* **2000**, *112*, 605; *Angew. Chem. Int. Ed.* **2000**, *39*, 592 – 595; f) C. Rocaboy, F. Hampel, J. A. Gladysz, *J. Org. Chem.* **2002**, *67*, 6863 – 6870; g) A.-M. Caminade, C.-O. Turrin, P. Sutra, J.-P. Majoral, *Curr. Opin. Colloid Interface Sci.* **2003**, *8*, 282 – 295.

[10] a) J.-M. Lehn, *Proc. Natl. Acad. Sci. USA* **2002**, *99*, 4763 – 4768; b) J. W. Goodby, *Curr. Opin. Colloid Interface Sci.* **1999**, *4*, 361 – 368; c) D. Guillon, R. Deschenaux, *Curr. Opin. Colloid Interface Sci.* **2002**, *6*, 515 – 525; d) T. Emrick, J. M. J. Fréchet, *Curr. Opin. Colloid Interface Sci.* **1999**, *4*, 15 – 23.

[11] a) H. Zimmermann, R. Poupko, Z. Luz, J. Billard, *Z. Naturforsch. A* **1985**, *40*, 149 – 160; b) J. Malthête, A. Collet, *Nouv. J. Chim* **1985**, *9*, 151 – 153; c) A.-M. Levelut, J. Malthête, A. Collet, *J. Phys.* **1986**, *47*, 351 – 357; d) J. Malthête, A. Collet, *J. Am. Chem. Soc.* **1987**, *109*, 7544 – 7545; e) R. Poupko, Z. Luz, N. Spielberg, H. Zimmermann, *J. Am. Chem. Soc.* **1989**, *111*, 6094 – 6105; f) H. Zimmermann, V. Bader, R. Poupko, E. J. Wachtel, Z. Luz, *J. Am. Chem. Soc.* **2002**, *124*, 15286 – 15301.

